Chinese Chemical Letters 36 (2025) 110555

Contents lists available at ScienceDirect

Chinese Chemical Letters

journal homepage: www.elsevier.com/locate/cclet

Steric effects and electronic manipulation of multiple donors on S_0/S_1 transition of D_n-A emitters

Shunyu Wang[a], Yanan Zhu[b,*], Yang Zhao[b], Wanli Nie[b], Hong Meng[a,b]

[a] School of Advanced Materials, Peking University Shenzhen Graduate School, Shenzhen 518055, China
[b] Faculty of Materials Science, Shenzhen MSU-BIT University, Shenzhen 518172, China

ARTICLE INFO

Article history:
Received 1 August 2024
Revised 10 October 2024
Accepted 15 October 2024
Available online 16 October 2024

Keywords:
Thermally activated delayed fluorescence
Donor-acceptor emitters
Structural relaxation
Stability
Steric hindrance
Reorganization energy

ABSTRACT

Multiple donor-acceptor (D-A) combinations represent a promising category of thermally activated delayed fluorescence (TADF) materials, offering potential for superior efficiency and stability. However, current systems are predominantly composed of limited donor groups, primarily carbazole-based derivatives. In this work, we developed a series of D-A type materials incorporating helical π-expanded carbazole (CzNaph) and 7*H*-dinaphtho[1,8-*bc*:1′,8′-*ef*]azepine (AzNaph), alongside traditional carbazole, ranging from mono- to tetra-substituted configurations (D_n-A). Through systematic investigation of geometric and electronic structures, the number and positioning of multiple donors are confirmed with significant manipulations on charge transfer characteristics and the S_1 state *via* steric effects. Density functional theory (DFT) calculations reveal that varying the number of π-extended donors within the acceptor framework produces emission colors from ultraviolet to red, providing a diverse range of emitters. Furthermore, the reduced reorganization energy of S_1 observed in tetra-substituted Cz and CzNaph, as well as MonoAzN, indicates lower structural relaxation, highlighting these materials' potential as stable luminescent candidates. This study underscores the importance of diverse composing units in achieving efficient and stable TADF emitters with multiple and hetero-donor configurations.

Thermally activated delayed fluorescence (TADF) materials are well known as the third generation of organic light-emitting diodes (OLEDs), *via* utilizing the reverse intersystem crossing (RISC) process induced by small singlet-triplet energy gap (ΔE_{ST}) [1-5]. Inspired by the pioneering work of Adachi *et al.* [1], a cascade of TADF emitters has been proposed to achieve high efficiency and full-color display in both academic and industry fields [6-8]. The concept of TADF molecular design originated from enlarging the spatial separation of the highest occupied molecular orbital (HOMO) and the lowest unoccupied molecular orbital (LUMO) [9,10], leading to the development of various categories of donor-acceptor (D-A) TADF emitters [7,11-16]. Recent research has prioritized the discovery of fluorescent emitters that exhibit both high RISC rates and intrinsic stability, addressing the commercial challenge of device longevity [17-19].

Beyond merely reducing the lifetime of triplet excitons through efficient RISC [20], the structural integrity of the emitters' core has been identified as a crucial determinant of luminescent lifespan [21], a long-standing and critical problem for TADF materials design [22,23]. Nevertheless, there remains a paucity of studies investigating the mechanisms underlying structural manipulation of excited states, particularly in D-A type TADF materials, upon exciton injection. For instance, carbazole-benzonitrile derivatives (CzBNs), such as the well-known 4CzIPN, featuring carbazole donors and benzonitrile acceptors, have demonstrated exceptional performance [1,7,21,22]. However, the relationships between stability, the variety and number of donors, geometric configurations, and the stability of radiative states have not been comprehensively elucidated.

From a chemical structure perspective, CzBNs emerge as promising candidates for high-efficiency, stable TADF OLEDs due to their multi-donor units that facilitate diverse D-A interactions and adjustable charge transfer (CT) strength. The intramolecular π-π interactions and delocalization effects are believed to significantly enhance their stability [23]. Recognizing the influence of multi-donor architectures, Duan *et al.* expanded the acceptor π-system with *para*-positioned π-conjugation tails, achieving impressive maximum external quantum efficiency (EQE_{max}) of 35.7% at 469 nm for CzBNs [7]. By leveraging the hetero-donor strategy, which involves incorporating secondary donor units to bolster stability [24,25], these derivatives have shown considerable improvements. However, many of these donors are carbazole-based,

* Corresponding author.
E-mail address: zhuyn@smbu.edu.cn (Y. Zhu).

https://doi.org/10.1016/j.cclet.2024.110555
1001-8417/

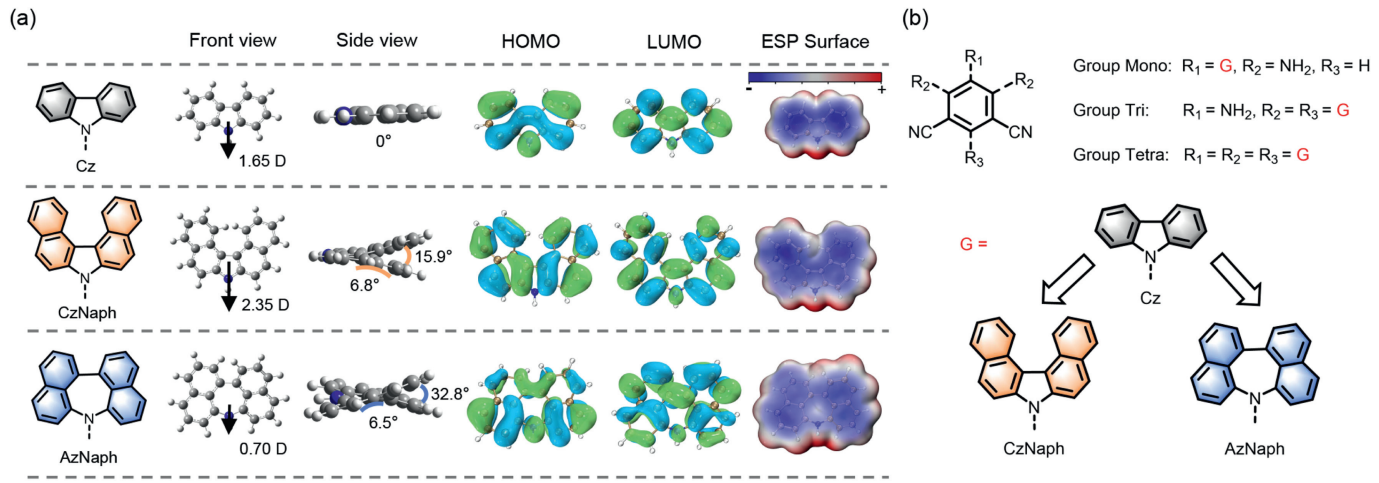

Fig. 1. (a) Geometric structures and fundamental electronic distribution of donors studied in this work. (b) Chemical structures of Group Mono/Tri/Tetra with studied π-extended carbazole derivatives.

such as parent carbazole and 3,6-disubstituted-carbazole [24,26-29]. Recent studies by Adachi *et al.* have validated the multiple and hetero-donor strategies by integrating various donor types [11]. Additionally, recent work has focused on replacing pentacyclic and hexacyclic rings with heptacyclic rings to create curved planes with negative curvature. This approach adjusts the characteristics of large planar systems, reduces intermolecular π-π interactions in conjugated systems, and enhances the stability of the system [30,31]. Our research group has also developed efficient and stable OLEDs based on heptacyclic ring molecules, introducing new donor [32] frameworks.

In this work, we introduce a series of multiple and hetero-donor type (D_n-A) molecules featuring three distinct donors (Fig. 1a), incorporating helical π-expanded carbazole (CzNaph) and novel heptacyclic azepine units (AzNaph) as extended fused moieties, as opposed to traditional single-linked carbazole (Cz) modifications. These donors are attached to a central phenyl ring, with varying acceptor groups, forming three distinct D-A material groups. The emitters based on these advanced donors demonstrate strong CT characteristics and reduced energy gaps between FMOs, attributed to the enhanced electron-donating properties and π-extended skeleton compared to traditional Cz donors. Additionally, the twisted structures of CzNaph and AzNaph introduce steric effects that impact the structural relaxation of excited states, thereby modulating the stability of the singlet state (S_1) based on the number and positions of substituents. By adjusting the number of π-extended donors with the acceptor moiety, the emission spectra of D_n-A compounds span from ultraviolet to red, offering versatile options for reference emitters. Notably, the reduced reorganization energy observed in the S_1 state of tetra-substituted Cz, CzNaph, and monoAzN compounds suggests less structural relaxation, indicating their potential as stable luminescent candidates. This work provides valuable insights into the underlying mechanisms of stability and the photophysical properties of these novel D_n-A materials, guiding the development of superior TADF emitters with multiple and hetero-donor configurations.

Towards the molecular design strategy for ideal TADF performance [24], employing a D-A system to form intramolecular CT states and spatial separation of the HOMO and LUMO for smaller ΔE_{ST}, we utilize π-expanded donors transitioning from Cz to CzNaph and AzNaph, as shown in Fig. 1a. Generally, conformational changes between S_1 and ground states should be suppressed to achieve good stability, typically achieved by a sterically crowded molecule. Additionally, forming a delocalized CT state with two or more donor units benefits the stability of excited states. Therefore, we presented and compared triple and tetra-substituted D-A materials with mono-donor frameworks to reveal the manipulation mechanism of multiple donors.

From the front view, these molecules enlarge the molecular skeleton and conjugation size *via* fused phenyl rings, exhibiting increasing polarity from Cz to CzNaph and indicating a rising charge transfer ability in related D_n-A emitters. However, the larger backbone size of AzNaph does not induce the dipole moment of the fragment due to the increasing intramolecular torsion between the naphthalene skeleton oppositely and the tension of the *quasi*-planar in the heptacyclic azepine core. Consistently, Cz exhibits almost planar configurations, while AzNaph shows torsion twice that of CzNaph, with a dihedral angle of 15.9°. Limited by the planar or *quasi*-planar backbone, the HOMO and LUMO are delocalized on the molecular skeleton. Conversely, the conjugation is slightly weakened by the out-of-plane dihedral torsions from Cz to CzNaph and AzNaph, as indicated by the electrostatic potential (ESP) map in the Fig. 1a. These phenomena, which seem contradictory, may introduce different manipulations on the properties of excited states.

Herein, we employ carbazole derivatives (Cz, CzNaph, and AzNaph) and benzonitrile (BN) derivatives as a versatile template to construct molecules (Fig. 1b). BN is well-recognized as a strong electron-accepting unit (A) with a high triplet energy level ($^3LE_1$) of 3.32 eV [23]. Conversely, Cz derivatives are frequently utilized as donor units (D), particularly in blue TADF emitters, due to their high $^3LE_1$ of 3.10 eV. The combination of these D and A units facilitates efficient electron transfer from the Cz derivatives to the BN derivatives, resulting in the formation of $^1CT_1$ (2.94 eV) and $^3CT_1$ (2.77 eV) states. Previous studies by Hosokai *et al.* [24] have demonstrated that the T_1 state of 5CzBN exhibits significant CT character, suggesting a predominant CT character over local excitation (LE) character in the T_1 state, as evidenced by the vibronic phosphorescence spectra.

Accordingly, we performed energy level calculations for these structures and the nine molecules composed of them, providing a detailed comparison of their electronic properties (Figs. 2a, c–e, Figs. S1 and S2 in Supporting information). Considering Cz, CzNaph, and AzNaph as donor units (D) and the remaining molecular components as acceptors (A), the following conclusions were drawn: Among the six parameters analyzed (ΔE_A^{HOMO}, ΔE_D^{HOMO}, ΔE_A^{LUMO}, ΔE_D^{LUMO}, ΔE_A^{Gap}, ΔE_D^{Gap}), with the exception of the HOMO relative to the acceptor segments, which shows a significant increase, most values are negative. This indicates that post-substitution, the overall energy gap, HOMO (spe-

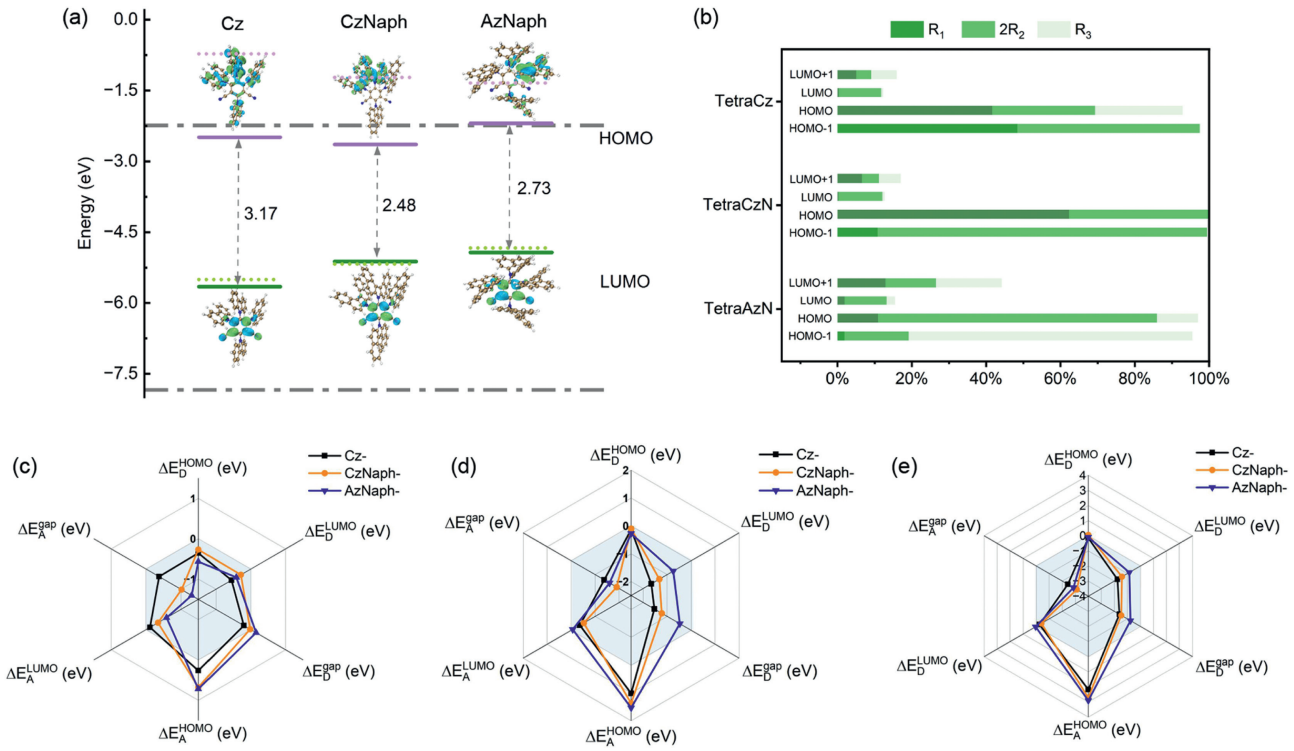

Fig. 2. (a) Frontier molecular orbitals (FMOs) energy comparison at ground states of Group Tetra. The HOMO (purple line) and LUMO (green line) of molecules are in solid lines, FMOs of π-extended carbazole derivatives (defined as donors) displayed in dash lines, where the gray dot-dash lines are the FMOs energy levels of acceptor core for each group. (b) The contributions of different substitution positions to the HOMO-1, HOMO, LUMO, and LUMO + 1 orbitals in the four tetra-molecules ($2R_2$ represents the sum of contributions from two groups at the R_2 position). (c–e) Represent the related energy difference between formed D_n-A and isolated D and A fragment, where $\Delta E_i^j = E_{D_n-A}^j - E_i^j$.

cific to the D fragment), and LUMO levels are reduced. In the D_n-A structures, the HOMO is predominantly localized around the donor segments, while the LUMO is centered near the acceptor core. As the number of donor substitutions increases, the variations in HOMO/LUMO energy levels converge towards zero, suggesting strong electron-donating characteristics of the D-fragments and potent electron-accepting capabilities of the A-core. This indicates pronounced charge separation characteristics within the molecules, with the overall energy level distribution primarily confined to the A-core (as indicated by the gray shaded area in the energy level diagram).

Further validation is provided through the analysis of the frontier molecular orbitals (FMOs) (Fig. 2b and Fig. S2 in Supporting information). In the four tetra-substituted molecules, the HOMO and HOMO-1 orbitals are predominantly contributed by the donor (over 90%), while the LUMO and LUMO+1 orbitals are primarily associated with the acceptor (over 80%). This clearly demonstrates the strong electron-donating nature of the donor segments and the electron-accepting strength of the acceptor segments, leading to CT characteristics in the excited state. Notably, the LUMO energy levels in AzNaph differ from the other three groups, potentially due to structural torsion impeding electron transfer. As the structural torsion increases from Cz to CzNaph to AzNaph, the donor contribution decreases, and the acceptor contribution to the increasing LUMO+1 levels. Additionally, the contributions to the FMOs from various donor sites were individually evaluated (Fig. 2b). At the HOMO level, the R_1 site shows the highest contribution (except in TetraAzN); at the LUMO level, the R_2 site dominates. In TetraCzN and TetraCzN, the contributions from the two R_2 sites are nearly identical, whereas in TetraAzN, significant differences exist, likely due to the large steric hindrance at the R_1 site introduced by the AzNaph group, disrupting molecular symmetry.

To explore the structure-property relationship affecting the emission performance of the D_n-A systems, electron-hole analyses [33] were conducted on the S_1 state of each molecule (Fig. 3a). Except for MonoCzN, which exhibits localized excitation (LE), all other molecules display delocalized charge transfer excitation (^{de}CT). In tri-substituted molecules, charge transfer predominantly occurs from the R_3 group to the central benzene ring, while in the AzN molecule, electrons transfer from the R_1, R_2, and R_3 groups to the center. This pattern is reversed in the tetra-substituted molecules: in TetraCz, holes are distributed across all four substitution sites, whereas in TetraCzN, holes are localized at the R_1 and R_2 positions, and in TetraAzN, holes are found at only one site.

We conducted structural optimization on the S_1 and T_1 excited state for each molecule, determining their energy levels, oscillator strengths (f), ΔE_{ST} and spin-orbit coupling (SOC) constant between S_1 and T_1 states (Fig. 3b and Table S3 in Supporting information). With an increasing number of substitutions, both of S_1 and T_1 energy level consistently decrease, following the trend Cz > CzNaph > AzNaph, and the ΔE_{ST} gradually decreases. Unlike the localized blue emission observed in previous multiple-donor emitters based on Cz [7,24], the emission wavelength shifts from blue to yellow due to the enhanced conjugation systems, which are progressively augmented by the increasing number of donors in D_n-A emitters (Figs. 3c–e). The decreasing S_1 energy levels correlate with the increasing number of donors and the enlarging donor skeleton size within each group. Notably, the newly introduced AzNaph, a non-Cz derivative, achieves the broadest emission spectrum, indicating the potential to realize a full-color spectrum through link modification.

However, the trend in emission strength, as indicated by the oscillator strength, does not align consistently with either the

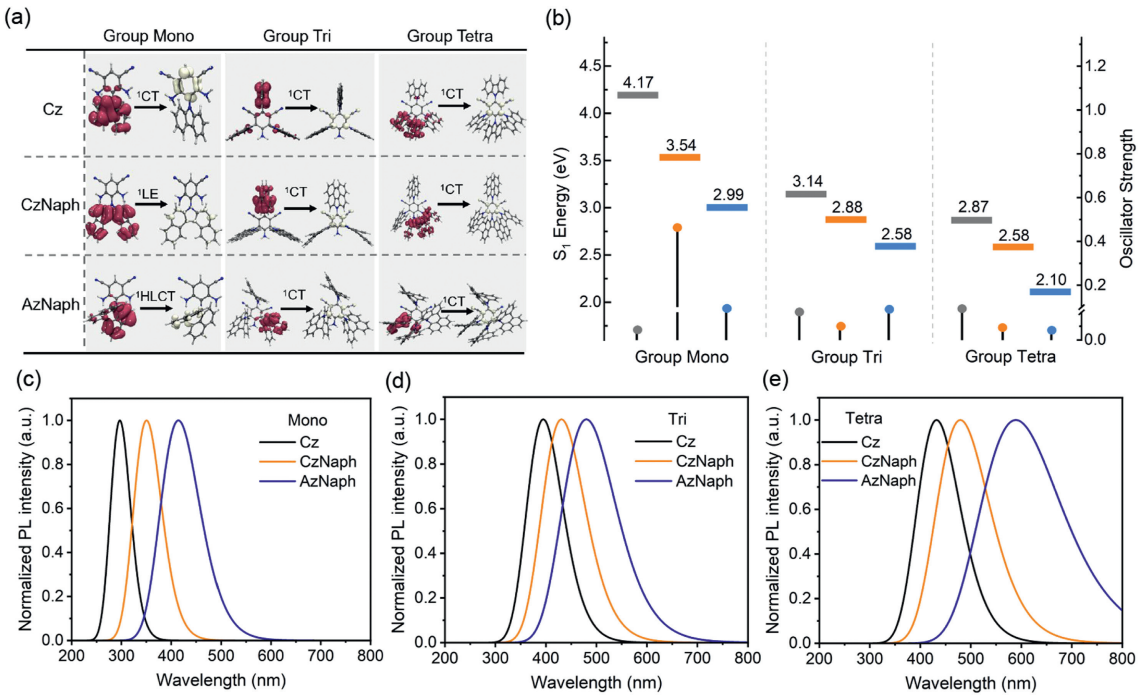

Fig. 3. (a) Hole and electron distributions at S_0-S_1 of studied molecules (red surface for holes, white for electrons), performed at ωB97x-D/6-31G**. (b) The predicted emission and oscillator strength (f) of S_1 states, where the gray, orange and blue solid line (dot) represented the donor named Cz, CzNaph and AzNaph consistent with Fig. 1a. (c–e) Calculated fluorescence spectra of studied molecules.

number or size of donors. Notably, CzNaph in the Group Mono exhibits the highest oscillator strength, which decreases rapidly as the number of CzNaph donors increases from $[CzNaph]_1$-A to $[CzNaph]_3$-A. Conversely, the emission strength increases steadily from Group Mono to Group Tetra when the donor in the D_n-A system is Cz, which has the smallest molecular size and the most planar structure. This observation aligns with previously reported data for 4CzIPN, known for its excellent performance in blue OLEDs as TADF emitters [1], but differs significantly when CzNaph is used as the donor. This suggests that the oscillator strength of emission diminishes with the aggregation of CzNaph donors, likely due to increased torsions (15.9°), reduced planarity. Conversely, with increased twisting and size in AzNaph (32.8°), steric effects create a hill trend in emission strength. Thus, it is essential to investigate the mechanism by which molecular size and steric torsions of multiple donors affect luminescence, particularly regarding emission strength and wavelength.

To further assess the impact of different donor torsion degrees (Fig. 4a) on molecular stability, we calculated the reorganization energies of these molecules (Fig. 4b). The decomposition modes (Fig. 4c) from S_0 to S_1 and from S_1 to S_0 are consistent across each structure; hence, subsequent analyses are based on the reorganization energy data from S_0 to S_1. By analyzing the projection ratios of the reorganization energy into three vibrational modes-stretch, bend, and dihedral vibrations—we observe consistent trends in both tri- and tetra-substituted molecules, with relatively larger values for Cz and AzNaph (Fig. 4d).

The reorganization energy of the AzNaph group is significantly higher than that of the other two groups, with CzNaph exhibiting the lowest value. There is a positive correlation between the dihedral contribution proportion and the overall magnitude of the reorganization energy. The structural torsion introduced by the heptacyclic ring in AzNaph results in the largest reorganization energy and dihedral fraction, indicating substantial conformational changes between the ground and excited states. This leads to the poorest stability and more pronounced non-radiative processes. In contrast, molecules containing five-membered rings, such as Cz and CzNaph, demonstrate better stability, with CzNaph being the most stable.

Further analysis of the vibrational modes in the three tetra-substituted molecules reveals that the low-frequency modes correspond to out-of-plane vibrations of the donor fragment, mid-frequency modes (around 1500 cm^{-1}) to in-plane stretching vibrations of the acceptor core, and high-frequency modes (around 2300 cm^{-1}) to in-plane stretching vibrations of the cyano group. These vibrational modes are present in all three molecules. However, while the absolute intensities of the mid- and high-frequency vibrations remain nearly unchanged, the intensity of the low-frequency modes increases in the order of CzNaph < Cz < AzNaph.

The significant reorganization energy at low frequencies suggests that these molecules may undergo structural inversions and changes at room temperature, impacting the properties of the excited state. This observation leads to the hypothesis that the excessively high reorganization energy at low frequencies in TetraAzN contributes to its instability. In contrast, TetraCz, with greater stability than TetraAzN, can undergo spin flips at room temperature under stable molecular conditions. Additionally, due to its higher SOC constant, the intersystem crossing (ISC) process in TetraCz occurs more readily, which is beneficial for its excellent TADF performance. In order to compare our molecules with similar molecules reported in recent years, we have performed extra calculations for seven molecules [7,23], including their S_1 energy levels and oscillator strengths. These data, along with the calculations for the three tetra-molecules, are included in Table S4 (Supporting information).

In this study, we designed a series of multi-donor type TADF emitters, systematically analyzing their structural and electronic properties to elucidate the effects of donor quantity and configuration on their photophysical behavior and stability. By incorporating various donor units into D-A compounds, we demonstrated that the introduction of multiple donor fragments enhances charge transfer characteristics and lowers the S_1 state energy. Our DFT calculations and electron-hole analyses further revealed that

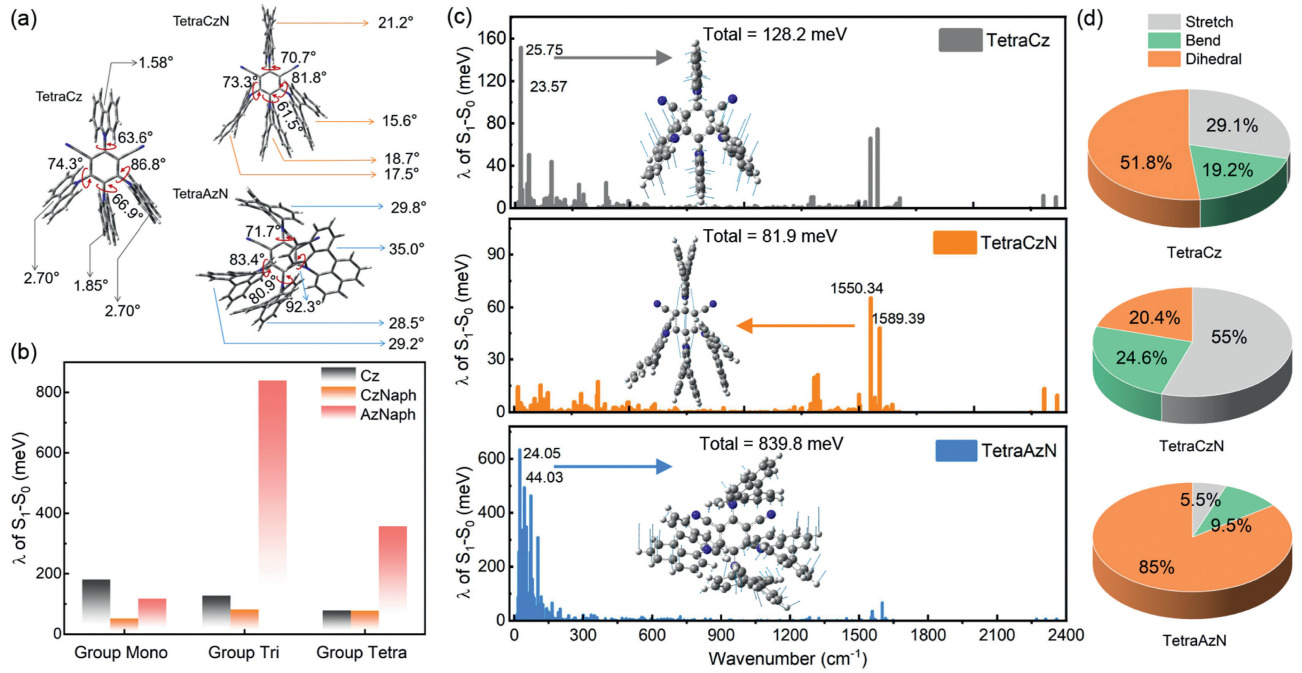

Fig. 4. Steric hindrance and structural relaxation decomposition in emission process of Group Tetra. (a) Torsion angles of intramolecular dihedrals. (b) Magnitude of the reorganization energy. (c) Vibrational mode analysis of the tetra-molecules during the S_0-S_1 transition. The ball-stick models inset represent the vibrational modes at the corresponding frequencies. (d) Projection of the reorganization energy onto three relevant vibrational modes with their respective contributions in percentages.

the increased structural torsion introduced by the heptacyclic ring exacerbates structural relaxation, thereby reducing emission efficiency. In contrast, the larger spatial potential resistance provided by the conventional five-membered-ring structure, particularly after π-expansion, enhances stability. This structural configuration allows TetraCzN to exhibit lower recombination energy compared to TetraCz. Consequently, when designing multi-donor type D-A TADF molecules, it is crucial to enhance the spatial site resistance while adequately controlling the structural torsion of the donor group to achieve materials with superior stability and luminescence properties. Our findings provide valuable insights into the design principles of TADF materials, underscoring the potential of multi-donor strategies in developing highly efficient and stable emitters for next-generation OLED applications.

Declaration of competing interest

The authors declare that they have no known competing financial interests or personal relationships that could have appeared to influence the work reported in this paper.

CRediT authorship contribution statement

Shunyu Wang: Writing – original draft, Visualization, Methodology, Formal analysis, Data curation, Conceptualization. **Yanan Zhu:** Writing – review & editing, Supervision, Funding acquisition, Conceptualization. **Yang Zhao:** Validation, Investigation, Formal analysis. **Wanli Nie:** Writing – review & editing, Validation. **Hong Meng:** Writing – review & editing, Supervision, Funding acquisition.

Acknowledgments

This work is financially supported by the National Key Research and Development Program of China (No. 2023YFB3608902), the National Natural Science Foundation of China (Nos. 22275003, 12404460), Key-Area Research and Development Program of Guangdong Province (No. 2019B010924003), Development and Reform Commission of Shenzhen Municipality (No. XMHT20220106002), Guangdong Key Laboratory of Flexible Optoelectronic Materials and Devices, the Foundation for Youth Innovative Talents in Higher Education of Guangdong Province (No. 2023KQNCX094), and the Guangdong Basic and Applied Basic Research Foundation (No. 2023A1515111072).

Supplementary materials

Supplementary material associated with this article can be found, in the online version, at doi:10.1016/j.cclet.2024.110555.

References

[1] H. Uoyama, K. Goushi, K. Shizu, H. Nomura, C. Adachi, Nature 492 (2012) 234–238.
[2] Y. Tao, K. Yuan, T. Chen, et al., Adv. Mater. 26 (2014) 7931–7958.
[3] Y. Liu, C. Li, Z. Ren, S. Yan, M.R. Bryce, Nat. Rev. Mater. 3 (2018) 18020.
[4] X. Tang, L.S. Cui, H.C. Li, et al., Nat. Mater. 19 (2020) 1332–1338.
[5] D. Zhou, W.P. To, Y. Kwak, et al., Adv. Sci. 6 (2019) 1802297.
[6] M. Hirai, N. Tanaka, M. Sakai, S. Yamaguchi, Chem. Rev. 119 (2019) 8291–8331.
[7] X. Hong, D. Zhang, C. Yin, et al., Chem 8 (2022) 1705–1719.
[8] M. Mahmoudi, D. Gudeika, S. Kutsiy, et al., ACS Appl. Mater. Interfaces 14 (2022) 40158–40172.
[9] J. Eng, T.J. Penfold, Chem. Rec. 20 (2020) 831–856.
[10] W. Ma, Y. Su, Q. Zhang, et al., Nat. Mater. 21 (2022) 210–216.
[11] B. Madushani, M. Mamada, K. Goushi, et al., Sci. Rep. 13 (2023) 7644.
[12] Y. Chen, D. Zhang, Y. Zhang, et al., Adv. Mater. 33 (2021) 2103293.
[13] H. Kaji, H. Suzuki, T. Fukushima, et al., Nat. Commun. 6 (2015) 8476.
[14] T.L. Wu, M.J. Huang, C.C. Lin, et al., Nat. Photonics 12 (2018) 235–240.
[15] Y. Kondo, K. Yoshiura, S. Kitera, et al., Nat. Photonics 13 (2019) 678–682.
[16] Y.L. Zhang, Q. Ran, Q. Wang, et al., Adv. Mater. 31 (2019) 1902368.
[17] Y. Zhu, S. Vela, H. Meng, C. Corminboeuf, M. Fumanal, Adv. Opt. Mater. 10 (2022) 2200509.
[18] L. Yao, S. Zhang, R. Wang, et al., Angew. Chem. Int. Ed. 53 (2014) 2119–2123.
[19] Y. Xu, P. Xu, D. Hu, Y. Ma, Chem. Soc. Rev. 50 (2021) 1030–1069.
[20] X. Song, S. Shen, M. Lu, et al., Chin. Chem. Lett. 35 (2024) 109118.
[21] H. Nakanotani, K. Masui, J. Nishide, T. Shibata, C. Adachi, Sci. Rep. 3 (2013) 2127.
[22] H.T. Feng, J. Zeng, P.A. Yin, et al., Nat. Commun. 11 (2020) 2617.
[23] T. Hosokai, H. Matsuzaki, H. Nakanotani, et al., Sci. Adv. 3 (2017) e1603282.
[24] C.Y. Chan, M. Tanaka, Y.T. Lee, et al., Nat. Photonics 15 (2021) 203–207.

[25] H. Noda, H. Nakanotani, C. Adachi, Sci. Adv. 4 (2018) eaao6910.
[26] Y.J. Cho, K.S. Yook, J.Y. Lee, Adv. Mater. 26 (2014) 6642–6646.
[27] Y. Zou, S. Gong, G. Xie, C. Yang, Adv. Opt. Mater. 6 (2018) 1800568.
[28] D. Zhang, X. Song, A.J. Gillett, et al., Adv. Mater. 32 (2020) 1908355.
[29] C. Yin, D. Zhang, L. Duan, Appl. Phys. Lett. 116 (2020) 120503.
[30] J.H. Jou, Y.C. Hsieh, H.H. Yu, et al., Org. Electron. 26 (2015) 285–291.
[31] J. Wang, F.G. Gamez, J. Marin-Beloqui, et al., Angew. Chem. Int. Ed. 62 (2023) e202217124.
[32] Z. Meng, Y. Zhu, H. Li, et al., J. Mater. Chem. C 12 (2024) 9993–9998.
[33] T. Lu, F. Chen, J. Comput. Chem. 33 (2012) 580–592.